Available online at www.sciencedirect.com

Remote Sensing of Environment 87 (2003) 377–388

Remote Sensing of Environment

www.elsevier.com/locate/rse

# Studies of land-cover, land-use, and biophysical properties of vegetation in the Large Scale Biosphere Atmosphere experiment in Amazônia

Dar A. Roberts[a,*], Michael Keller[b,c], João Vianei Soares[d]

[a] Department of Geography, EH3611, University of California, Santa Barbara, CA 93106, USA
[b] USDA Forest Service, International Institute of Tropical Forestry, San Juan, Puerto Rico
[c] Complex Systems Research Center, University of New Hampshire, Durham, NH, USA
[d] Instituto Nacional de Pesquisas Espaciais, OBT/SERE, Avenida dos Astronautas, 1758, 12245-970 São José dos Campos, SP, Brazil

Received 6 July 2003; received in revised form 4 August 2003; accepted 5 August 2003

## Abstract

We summarize early research on land-cover, land-use, and biophysical properties of vegetation from the Large Scale Biosphere Atmosphere (LBA) experiment in Amazônia. LBA is an international research program developed to evaluate regional function and to determine how land-use and climate modify biological, chemical and physical processes there. Remote sensing has played a fundamental role in LBA in research planning, land-cover mapping and in long-term monitoring of changes in land-cover and land-use at multiple scales. This special issue includes 12 papers that cover a range in spatial scales from regional mapping to local scales that cover only a portion of a Landsat scene. Several themes dominate, including land-cover mapping with an emphasis on wetlands and second-growth forest, evaluation of pasture sustainability and forest degradation and the impact of land-cover change on stream chemistry. New techniques introduced include automated Monte Carlo unmixing (AutoMCU) and several new approaches for mapping land-cover. A diversity of sensors are utilized, including ETM+, IKONOS, SPOT-4, Airborne P-band synthetic aperture radar (SAR), and L-band SAR. Census data are fused with an existing land-cover map to generate spatially explicit estimates of land-use from historical data. Several papers include important, new field measures of species composition, forest structure and biomass in mature forest and secondary succession.


*Keywords:* LBA; Amazônia; Brazil; Cerrado

## 1. Introduction

The Large Scale Biosphere Atmosphere (LBA) experiment in Amazônia is an international research program led by Brazil designed to investigate how the Amazon region functions as part of the Earth system, and to evaluate how changes in land-use and climate may modify biological, chemical and physical processes. Ecological studies within the program focus on addressing the key question:

> How do tropical forest conversion, regrowth, and selective logging influence carbon storage, nutrient dynamics, trace gas fluxes, and the prospect of sustainable land-use in Amazônia?

LBA planning began in 1993 (Avissar & Nobre, 2002), and field research began in 1998. Seven scientific themes are emphasized in LBA: (1) land-use land-cover change, (2) physical climate, (3) carbon dynamics, (4) biogeochemistry, (5) atmospheric chemistry, (6) land surface hydrology and aquatic chemistry, and (7) human dimensions.

The Amazon River Basin covers an area of nearly 6 million km$^2$, including the largest remaining area of primary forest globally and the world's largest river (Salati & Vose, 1984). Because of the large area, poor access and need for historical and current information on land cover, remote sensing has played a fundamental role in preparation and implementation of LBA. This special issue presents a cross-section of much of the remote sensing research that has occurred over the past few years in support of this program.

This special issue includes 12 papers that range in scale from region-wide to local and cover topics ranging from land-cover classification to biophysical characterization and

* Corresponding author. Tel.: +1-805-893-2276; fax: +1-805-893-3146.
*E-mail address:* dar@geog.ucsb.edu (D.A. Roberts).

0034-4257/$ - see front matter © 2003 Elsevier Inc. All rights reserved.
doi:10.1016/j.rse.2003.08.012

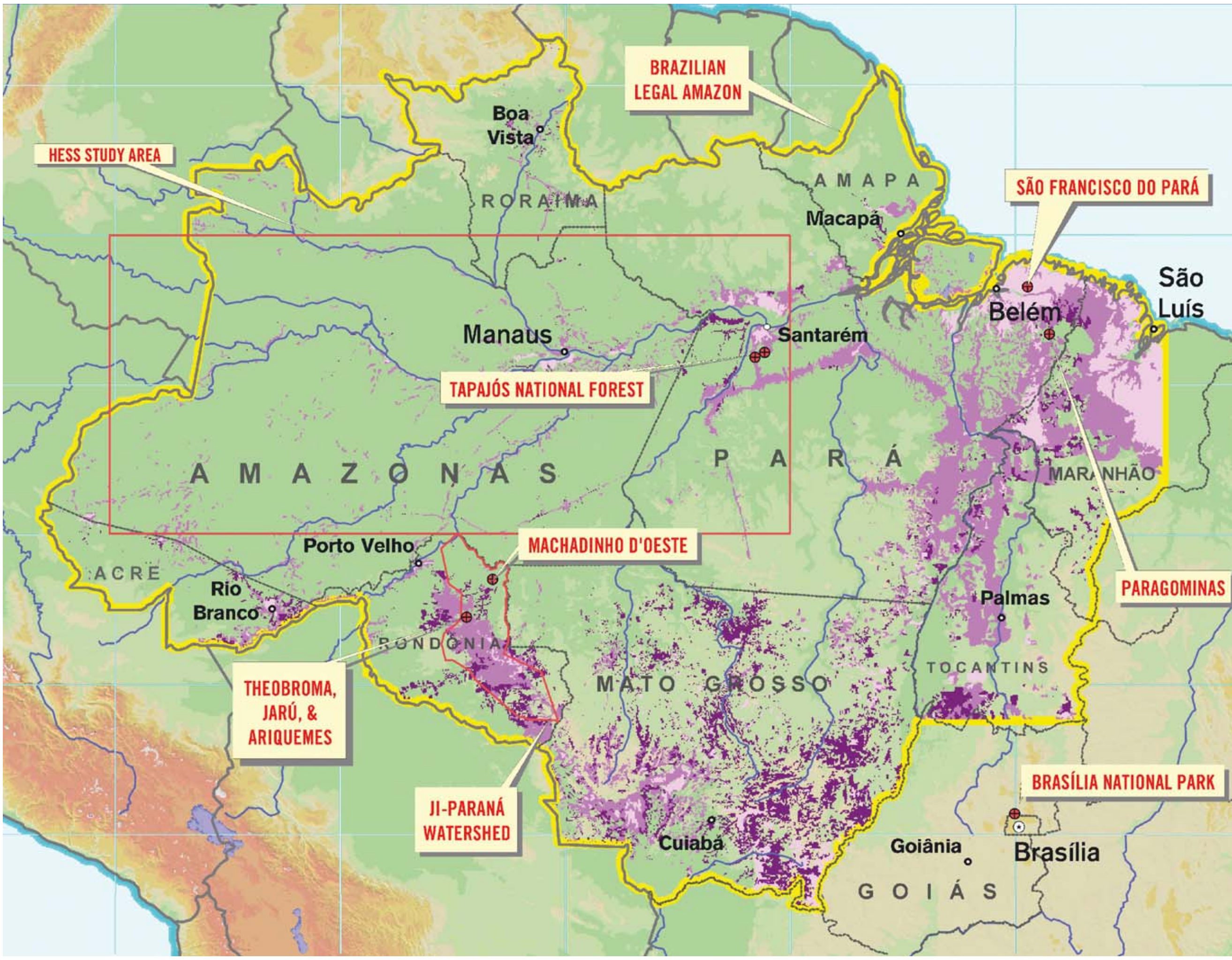


Fig. 1. Index map showing the outline of the Brazilian Legal Amazon (yellow), and the location of study sites described in the special issue. The 18 × 8° study area described by Hess et al. (2003) is outlined in red. Areas marked in pink, magenta and dark purple represent areas of old (1971–1977), intermediate (1977–1987), and more recent deforestation (1988–1991). The cleared area along the southwestern and southern flanks of the Brazilian Legal Amazon is commonly referred to as the Arc of Deforestation.

land-use change (Fig. 1; Table 1). While LBA considers the whole Amazon region, research in the special issue falls within the Brazilian Legal Amazon with the exception of the work near Brasília (Fig. 1). Although a large number of subsidiary questions guide ecological research in LBA (see Keller et al., in press), the primary focus of the papers in this issue is land-cover/land-use change (Table 1). This article provides a brief overview of the physical setting, a background on remote sensing research in the Amazon and a brief summary of the articles included in this special issue.

## 2. Background

### 2.1. Physical setting

The Legal Amazon region of Brazil, as shown in Fig. 1, covers an area of 5.8 million km$^2$, consisting primarily of closed tropical forest, but also including large areas of flooded forest and *cerrado* (savanna). Approximately 15% of the forests of the Brazilian Legal Amazon have been cleared in the past 30 years (Houghton et al., 2000). Average temperature within the region varies from 25.8 °C in the wet season to 27.9 °C in the dry season (Junk & Firch, 1985). Annual rainfall averages approximately 2150 mm, but varies considerably, ranging from 1500 mm in the north and south to over 3500 mm in the northwest (INMET, 1999). Most areas experience seasonal variation in precipitation, with the start and end of the rainy season varying by over a month, starting earliest in the south in October and latest in the north in December and typically extending 7 months (Junk & Firch, 1985). Persistent cloud cover is just one of many factors that limit the timing and types of remotely sensed data used. Most fine spatial resolution optical data sets are acquired during the dry season, while synthetic aperture radar (SAR) has been used throughout the year.

Table 1
List of authors, general study location and topics

| Authors | Location | Topic |
|---|---|---|
| Siqueira et al. | Region-wide | Land-cover mapping using dual season SAR |
| Hess et al. | Central Amazon Region | Mapping of flooded forest and inundation |
| Ballester et al. | JiParaná, Rondônia | Land cover/Land use and water chemistry |
| Numata et al. | Rondônia | Land-cover characterization, nutrient dynamics in pastures |
| Lu et al. | Machadinho, Rondônia | Secondary forest |
| Vieira et al. | Zona Bragatina, Pará | Secondary forest |
| Santos et al. | Tapajós, Pará | Biomass retrieval, P-Band SAR, Secondary forest |
| Souza et al. | Paragominas, Pará | Forest degradation, land-cover mapping |
| Asner et al. | Tapajós, Pará | Biophysical remote sensing |
| Asner and Warner | Region-wide, local | Biophysical remote sensing of forest structure |
| Ferreira et al. | Brazilian Cerrado | Seasonal dynamics, sensor evaluation |
| Cardille and Foley | Region Wide | Land-use change |

Two defining properties of the Amazon region include the recycling of evapotranspired moisture and the large area of the region that is either permanently or periodically flooded. Between 63% and 73% of the annual rainfall is evapotranspired (Marengo & Nobre, 2001), with approximately 50% recycled in the region as rainfall (Salati, 1985), implying that deforestation may significantly modify regional, and potentially global hydrology (Lean & Rowntree, 1993; Nobre, Sellers, & Shukla, 1991). Hess, Melack, Novo, Barbosa, and Gastil (2003) estimate that 17% of central Amazônia is occupied by wetlands, with 96% inundated at high water in 1996 and 26% inundated at low in 1995.

Although the region has a very long history of human habitation, major conversion of forest to agricultural lands is restricted primarily to the last 30 years, with most deforestation concentrated along the southern and eastern flanks of the region, in an area termed the ‘‘arc of deforestation’’ (Fig. 1). Many of the local study sites represented in this special issue, including Paragominas and Rondônia fall within this arc of deforestation. The zona Bragantina, described by Vieira et al. (2003), is the site of some of the earliest agricultural colonization projects in the Brazilian Amazon.

One primary motivating factor for research is the extent to which land-cover change and subsequent land-use impact the global carbon budget. Houghton, Lawrence, Hackler, and Brown (2001), estimate that Amazonian vegetation contains 70 Pg of carbon, accounting for 10–15% of the global biomass. Land-cover conversion releases much of this carbon and thus may account for a significant proportion of the terrestrial flux of carbon to the atmosphere. In contrast to deforestation, pasture abandonment and forest regeneration potentially represents a substantial carbon sink (Brown & Lugo, 1992). The amount of cleared lands that have been abandoned and are regenerating is not exactly known, but has been recently estimated to be as much as 35.8% (Lucas, Honzak, do Amaral, Curran, & Foody, 2002).

While rates of deforestation are estimated annually by Brazil’s National Institute for Space Research (INPE), and many recent studies have focused on mapping the extent of second-growth forest, a third form of land modification, termed forest degradation, has only recently been recognized as significant. Forest degradation, defined as the combined effects of fire, fragmentation and selective logging, may exceed deforestation on an areal basis (Nepstad et al., 1999), especially during El Niño years. While the extent of degraded forests is under debate, the area is potentially quite large. For example, Nepstad et al. (1999) estimated annual rates of degradation of over 120,000 km$^2$, with 8000–15,000 km$^2$ due to logging, up to 80,000 km$^2$ due to burning and up to 38,000 km$^2$ due to fragmentation. In contrast, deforestation rates have averaged between 18,000 and 19,000 km$^2$/year since 1978, with a range of 11,000–29,000 km$^2$/year (INPE, 2000), equaling slightly over 18,000 km$^2$/year in the newest assessment done by INPE for 2001 (Table 2; INPE, 2003). The potential impact of forest degradation on carbon remains a major research question.

### 2.2. Remote sensing

Remote sensing has played an important role in mapping land-cover and quantifying change in Amazônia for more than 25 years. Land-cover classification represents one of the most fundamental applications of remote sensing, and is widely used to estimate carbon stocks (i.e., Houghton et al., 2000) and parameterize hydrological and biogeochemical models (e.g., Potter et al., 1993; Running et al., 1999).

Table 2
Deforestation rates, in square kilometers/year [www.dpi.inpe.br/prodesdigital, INPE, 2003]

| State | Deforestation 2000–2001 |
|---|---|
| Acre | 419 |
| Amapá | 7 |
| Amazonas | 634 |
| Maranhão | 958 |
| Mato Grosso | 7703 |
| Pará | 5237 |
| Rondônia | 2673 |
| Roraima | 345 |
| Tocantins | 189 |
| Amazônia | 18,166 |

Numerous region-wide maps have been produced using a diversity of sensors including the radar-based RADAM-BRASIL, several developed using 1 km resolution Advanced Very High Resolution Radiometer (AVHRR) time series data (Hansen, Defries, Townshend, & Sohlberg, 2000; Loveland et al., 2000; Stone, Schlesinger, Houghton, & Woodwell, 1994), and most recently, a 1-km resolution single-season (Saatchi, Nelson, Podest, & Holt, 2000) and dual-season (Siqueira, Chapman, & McGarragh, 2003) mosaic of Japanese Earth Resource Satellite-1 (JERS-1) data. Landsat Multispectral Scanner (MSS) and Thematic Mapper (TM) have been used for regional studies of deforestation in Brazil (Houghton et al., 2000; INPE, 2000, 2003; Skole & Tucker, 1993) and in other Amazon region countries (Hansen et al., 2000). Finer-scale mapping has focused primarily on the use of Landsat TM data applied at local scales, ranging from a portion of a Landsat scene (Adams et al., 1995; de Moraes, Seyler, Cerri, & Volkoff, 1998; Moran, Brondizio, Mausel, & Wu, 1994; Roberts, Batista, Pereira, Waller, & Nelson, 1998) to several contiguous scenes (Ballester et al., 2003; Roberts et al., 2002). Although most remote sensing studies have focused on the Brazilian Amazon, a few recent studies have occurred outside of Brazil (e.g., Steininger et al., 2001).

One of the greatest strengths of remote sensing is its ability to image the same region multiple times and thus quantify change. With a satellite record extending back to 1972, Landsat data provide over 30 years of observations, thus capturing the period of time in which the greatest changes in land-cover have occurred in Amazônia. More recent research has begun to take advantage of more advanced spaceborne capabilities, such as the very fine spatial resolution of IKONOS (1 m panchromatic, 4 m multispectral) (Asner & Warner, 2003) and hyperspectral imaging of Hyperion. The use of coarse resolution data acquired by meteorological satellites such as AVHRR, and more recently the Moderate-Resolution Imaging Spectroradiometer (MODIS), have extended this analysis to include a fine temporal sampling, thus providing the ability to screen out clouds and capture seasonal dynamics within the region. Passive and active microwave sensors, including the Scanning Multichannel Microwave Radiometer (SMMR), Shuttle Imaging Radar (SIR-C), Radarsat and JERS-1 provide all-weather imaging at a range of spatial and temporal scales, from coarse resolution, daily measurements (SMMR), to infrequent, fine spatial resolution SAR.

Some of the earliest applications of remote sensing in Amazônia, focused on quantifying rates of deforestation using historical Landsat MSS (Fearnside & Salati, 1985), AVHRR (Malingreau & Tucker, 1990) and Landsat MSS and TM (Skole & Tucker, 1993; INPE, 2000, 2003). Using these data, annual rates of deforestation have been shown to vary considerably locally and temporally, ranging from a low of 11,000 $km^2$/year between 1990 and 1991 (Fearnside, 1993) to a high of 29,000 $km^2$/year in 1995 (INPE, 2000, 2003). While confidence in estimates of deforestation rates have improved, considerable uncertainty remains in estimated carbon fluxes because of the uncertainty in biomass estimated for primary forest (Brown et al., 1995; Houghton et al., 2000).

More recent research has focused on the fate of lands after they have been cleared. Much of this research has concentrated on mapping areal extent, age and persistence of secondary forest (Alves, Pereira, De Sousa, Soares, & Yamaguchi, 1999; Angelis, Freitas, Valeriano, & Dutra, 2002; Foody, Palubinskas, Lucas, Curran, & Honzak, 1996; Kimes, Nelson, Salas, & Skole, 1999; Lucas et al., 2002; Lucas, Honzak, Foody, Curran, & Corves, 1993; Moran et al., 1994; Nelson, Kimes, Salas, & Routhier, 2000; Rignot, Salas, & Skole, 1997; Roberts et al., 2002; Salas, Ducey, Rignot, & Skole, (2002a, 2002b); Skole, Chomentowski, & Salas, 1994; Steininger, 1996). Three papers in this special issue focus on secondary forest (Table 1). Interest in secondary forest has been generated by its potential as a carbon sink (Brown & Lugo, 1992). However, definitions, methods and areal estimates differ considerably at local and regional scales (Fearnside, 1996; Lucas et al., 2000; Moran et al., 1994; Roberts et al., 2002). Furthermore, carbon uptake rates have been found to vary considerably depending upon prior land-use and soil quality (Alves et al., 1997; Johnson, Zarin, & Johnson, 2000; Lucas et al., 2002; Moran et al., 2000).

Forest degradation, although initially described over 10 years ago (Uhl & Vieira, 1989) has only recently been identified as a potential major source of land-cover change (Nepstad et al., 1999). A number of studies have used remote sensing to map logged (Asner, Keller, Pereira, & Zweede, 2002; Asner, Keller, Pereira, Zweede, & Silva, in press; Pereira, Zweede, Asner, & Keller, 2002; Souza & Barreto, 2000; Stone & Lefebvre, 1998) and burned forest (Cochrane & Souza, 1998). Forest fragmentation is widely recognized as a potential source of biodiversity loss (e.g., Laurance, Ferreira, Rankin-de Merona, & Laurance, 1998; Skole & Tucker, 1993) and may act synergistically to increase burning in forests (Cochrane, 2001). In this issue, Souza et al. describe a new approach for mapping forest degradation in Paragominas. Microwave remote sensing has been used to map and classify wetlands in the Amazon region. Sippel, Hamilton, Melack, and Choudhury (1994) utilized SMMR data to map seasonal and long-term changes in flood extent along the Amazon main stem. Hess, Melack, Filoso, and Wang (1995) used SIR-C data to discriminate a number of wetland-cover types using a decision tree classifier. Novo, Costa, Mantovani, and Lima (2002) combined Radarsat C-band and JERS-1 L-band to map flooded macrophytes in the Tucurui reservoir, while Costa, Niemann, Novo, and Ahern (2002) used a similar data set to monitor seasonal changes in radar backscatter associated with the flood cycle. In this issue, Hess et al. map wetland vegetation over a large area of central Amazônia using a dual season mosaic of JERS-1 data described by Siqueira et al. (2003).

## 3. Summary of papers

A majority of the papers submitted to the special issue can be placed into three broad categories, land-cover mapping, land-cover characterization and land-use change (Table 1). The spatial scale of the studies varied from region-wide (Siqueira et al., 2003; Cardille & Foley, 2003) to an area less than 1600 $km^2$ (Lu, Moran, & Batistella, 2003). In the following section, we provide a brief summary of each paper and place the research within the broader context of Amazonian research. We have organized the discussion into the three broad topics and ordered them from large scale to more local scale studies. The locations of regional and local study locations are shown in Fig. 1.

### *3.1. Land-cover mapping*

Siqueira et al. (2003) describe the creation of a dual season mosaic of JERS-1 LHH data at 100-m resolution. The mosaic, which was created from imagery acquired at low water in September/October 1995 and high water between May and June, 1996, is unique because it captures the main stem Amazon and its tributaries during two flood extremes, events that could only be observed using a cloud-penetrating radar system such as JERS-1. To demonstrate some of the utility of the mosaic, dual season backscatter was used to generate a land-cover map using a simple threshold classifier. Region-wide estimates of land-cover showed large areas of flooded vegetation and open water in Amazonas and Pará. To evaluate their map at a diversity of scales, areal estimates of forest, non-forest and water were compared to estimates by Skole and Tucker (1993) for nine Brazilian states, Rondônia (Roberts et al., 2002) and in an area near Manaus (Hess et al., 1995). These comparisons showed a generally good correspondence, although the simple classifier employed tended to underestimate cleared areas.

Hess et al. (2003) provide an excellent example of the utility of the dual season JERS-1 mosaic. The authors describe a two stage procedure for classifying these data into a map of wetland vegetation communities, in which image segmentation was used to generate a wetlands mask, followed by a decision tree classifier applied to high and low water data to map five wetland classes at two flood states, open water and two other specialized classes. Classes adhered to national map standards and are valuable for biogeoghemical modeling in wetland areas. The procedure was applied to an $18 \times 8°$ east–west subset of the JERS-1 mosaic (Fig. 1). Accuracy was assessed using digital airborne videography acquired at high and low water between 1995 and 1999 (Hess et al., 2002). Detailed examples of high and low water classified maps were provided for a range of geomorphologically distinct flood plains. Analysis of discharge and rainfall, derived from 28 gauges distributed across the network suggest that extreme flood states (high and low) were adequately captured by the mosaic.

This study demonstrates the very important role of wetlands in the Amazon region. The authors found that 17% of the $18 \times 8°$ subset of the JERS-1 mosaic was classified as wetland. Of this area, 96% was inundated at high water in 1996, and 26% at low water in 1995. Flooded forest constituted nearly 70% of the entire wetland. This area is significantly larger than the wetlands mapped in the most commonly used global land-cover maps (e.g., Loveland et al., 2000). Recent work by Richey, Melack, Aufdenkampe, Ballester, and Hess (2002), using this wetland map to estimate $CO_2$ flux from surface waters in the central Amazon, suggests that $CO_2$ outgassing from wetlands and rivers accounts for 0.5 Pg C $year^{-1}$.

Several papers describe more local efforts to map land-cover. Ballester et al. (2003) integrate GIS and remote sensing to evaluate the impact of land-use and land-cover on stream chemistry in the Ji-Paraná Basin, a watershed covered by eight Landsat scenes (Fig. 1). To evaluate the intensity of land-use, four categories were established based on the area cleared, low (0–15%), medium (15–30%), high (30–50%) and very high (50–75%). Water chemistry was sampled from each drainage unit including $Ca^{2+}$, $Mg^{2+}$, $Na^{+}$, $K^{+}$, $Cl^{-}$, and soluble reactive $PO_4^{3-}$. Watershed characteristics were derived from a digital elevation model and soil chemistry was determined from the EMBRAPA and SIGTERON databases (Cochrane & Cochrance, 1998; EMBRAPA, 1983), and used to derive soil $Ca^{2+}$, $Mg^{2+}$, $Na^{+}$, $K^{+}$, $H^{+}$, $Al^{3+}$, and effective cation exchange capacity (ECEC). Supervised classification was used to map eight land-cover classes. Accuracy was assessed using digital videography and field data. The importance of various environmental/land-use controls on stream chemistry was evaluated using multiple regression.

The authors demonstrated fairly high classification accuracy, with the greatest source of error being confusion between pasture and secondary forest. Mature forest and pasture constituted greater than 93% of the watershed, with only 3.9% mapped as secondary forest and approximately 2% within other classes. Broad categories of low, intermediate and high ionic concentration in rivers matched patterns of deforestation and soils. Areas with the most nutrient-poor soils and least deforestation had the lowest ionic concentration, whereas areas with the most nutrient-rich soils and highest pasture area had the highest ionic concentrations. Pasture area and ECEC in soils were both good predictors of river chemistry.

This study is notable because it reports a strong association between pasture area in Rondônia and the distribution of nutrient-rich soils, finding pasture area as a good predictor of stream chemistry. Similar findings are reported by Biggs, Dunne, Domingues, and Martinelli (2002), who also found a strong association between pasture area and nutrient-rich soils. However, in that study the authors concluded that best predictor of stream chemistry was the soil, not pasture area. The proportion of cleared lands abandoned to secondary forest reported by Ballester et al.

(2003) is potentially the lowest in the Brazilian Amazon region. For example, Lucas et al. (2002) using AVHRR, estimated that 35.8% of cleared lands between 1991 and 1994 were in secondary forest, whereas Fearnside (1996) estimated approximately 47%. Moran et al. (1994) reported some of the highest values, estimating the proportion of secondary forest to cleared area at 46% for Western Altimira in 1985 with a high of 82% for the same area in 1991. Skole et al. (1994), reported 30% for Rondônia, while Roberts et al. (2002), reported an average of 22% for two Landsat scenes located in the central portion of that state. Local and region-wide differences in estimates of secondary forest highlight the challenge of mapping this dynamic land-cover class.

Two other studies in the special issue focus on the state of Rondônia. Numata et al. (2003), evaluate the potential of remote sensing for assessing pasture soil fertility, whereas Lu et al. (2003) describe a new approach for mapping second-growth forest using Spectral Mixture Analysis (SMA). Numata et al. (2003) analyzed pasture chronosequences in Rondônia, calculating Normalized Difference Vegetation Index (NDVI) and fractions of non-photosynthetic vegetation (NPV), green vegetation (GV), soil and shade using SMA. Three study sites, covering a range in soil nutrient availability were studied in the field for pastures aged 1–2, 3–5, 6–10, and >10 years. Aggregated soil samples were analyzed for P, K, Ca, Mg, Al, ECEC, and base saturation.

Based on image analysis, pastures demonstrated a strong time-dependent change in physical properties, showing a general increase in NPV and decrease in GV and shade with age. Soil P, base saturation, and Ca decreased with increasing pasture age, while ECEC showed an initial increase followed by a decrease at one site. Remotely sensed measures were most responsive to soil P, with the highest negative correlation occurring between NPV and P at the most nutrient-rich site. Similar findings were published by Asner, Townsend, and Bustamante (1999), who observed a strong correlation between the NPV Index and soil P and Ca along a pasture chronosequence near Santarém, Pará. However, no consistent relation was observed by Numata et al. (2003) at all sites, with the poorest relations observed for the site with the lowest nutrient availability. Important observations include age-dependent changes in canopy structure in pastures, characterized by increased NPV, decreased GV and shade and the demonstration that Landsat TM is capable of assessing pasture nutrient status, at least in nutrient-rich soils.

Lu et al. (2003) evaluate methods for mapping second-growth forest using Landsat TM acquired in northern Rondônia, in the vicinity of Machadinho. Secondary forest was divided into three classes: early regeneration (SS1), intermediate (SS2) and advanced (SS3), defined from structural parameters determined in the field, but not stand age. Accuracy was assessed through a combination of field plots and IKONOS imagery.

Four classification approaches were compared, one based on a standard Maximum Likelihood Classifier (MLC) applied to the original TM bands, and the other three based on fractions derived using a linear mixture model. Analysis of spectral fractions demonstrated a general increase in shade and decrease in GV with more advanced stages of second growth. When comparing classification approaches the highest accuracies were observed for secondary forest mapped using a threshold applied to the ratio of shade over GV with the lowest accuracy produced using the MLC applied to TM bands. The greatest confusion occurred between successional stages. The paper highlights the importance of shade as a discriminator of secondary forest.

Vieira et al. (2003) also focus on the issue of mapping second-growth forest. They describe a detailed field/remote sensing study in the São Francisco Municipality, located approximately 110 km east of the city of Belém (Fig. 1). This region is unique because it that has experienced over 100 years of human settlement and includes some of the oldest agricultural colonies in the Brazilian Amazon. For remote sensing, secondary forest was classified into three age classes, young (3–6 years), intermediate (10–20 years) and advanced (40–70 years). Landsat 7 data were used to map the areal extent of secondary forest age classes, mature forest, tree crops, pasture and row crops/soil. Field data were collected from 16 plots, four in mature forest, and a pair in 3-, 6-, 10-, 20-, 40- and 70-year-old stands. Field measures included total biomass, height, diameter at breast height (DBH), basal area, leaf area index (LAI), plant density and species composition, which were determined for each plot and used to compare structural and compositional differences between different aged stands.

Overall classification accuracy based on 94 field sites was high with the greatest confusion between tree crops and initial succession. The best separation between second-growth age classes was observed in TM band 5, with NDVI showing little separability between age classes. Biomass inventories showed these stands to have some of the lowest biomass accumulation rates described in the Amazon region, ranging from a low of 2.1 Mg/ha for a 3-year-old stand (below 1 Mg/ha/year) to 141 Mg/ha for a 70-year-old stand (average 2 Mg/ha/year). The distribution of biomass changed dramatically with age, with more than 50% of the biomass in foliage for stands younger than 10 years, decreasing to 33% by 20 years and less than 6% in mature forest. Species composition was most similar for the youngest stands (< 20 years old) and oldest stands (40–70 years) based on the Sorenson Index.

The potential of second growth as a carbon sink, and the extent to which large areas of cleared lands have reverted to second growth have focused considerable interest in mapping this class. Inconsistent definitions of second growth, differences in mapping techniques and the dependence of carbon sequestration rates on prior land-use and soil quality (Alves et al., 1997; Lucas et al., 2002; Moran et al., 2000) complicate efforts to use maps of second growth to estimate carbon stocks and fluxes. The low biomass accumulation rates published by Vieira et al. (2003) highlight the importance of taking into account regional differences in soil quality and land-use history. For example, Alves et al. (1997) report biomass values ranging between 73 and 163 Mg/ha for 11- to 18-year-old stands in Rondônia. Even higher values are reported for areas near Manaus, with values as high as 200 Mg/ha for a 20-year-old stand and as high as 70 Mg/ha for one 5-year-old stand (Steininger, 2000). By comparison, the 20-year-old stand reported by Vieira et al. (2003) had a biomass of 51.9 Mg/ha and even the 70-year-old stand did not exceed 150 Mg/ha.

Second growth and associated biomass is also the focus of Santos et al. (2003). This paper could be considered both an application of remote sensing to map land-cover as well as an application of remote sensing to retrieve a biophysical property. Santos et al. analyze P-band polarimetric data acquired in the vicinity of the Tapajós National Forest to evaluate the potential of P-band SAR for biomass retrievals. Radar backscatter was compared to biomass estimated in the field from forest inventories for primary forest, initial (< 5 years), intermediate (5–15 years) and advanced succession (>15 years). To scale up point measurements to the region, the backscatter data were classified into six land-cover classes using the contextual classifier, ICM.

They report mature forest biomass ranging between 152.8 and 271.8 Mg/ha. Advanced succession ranged between 63.8 and 111.6 Mg/ha, followed by intermediate succession (22.6–35.5 Mg/ha) and young succession (5.3 to 16.1 Mg/ha). P-band backscatter was fit to a third-order polynomial and a logarithmic function. Polarimetric data showed lowest backscatter in VV followed by HH and HV. Based on model fits, radar backscatter saturated at slightly above 50 Mg/ha. High levels of classification accuracy were achieved using the ICM classifier with the greatest confusion occurring between advanced succession and mature forest. Considerable confusion also occurred between various age classes of secondary succession. This paper is significant because it reports on some of the first use of Polarimetric P-band SAR in Amazônia. Moderate levels of saturation at 50 Mg/ha, suggest that P-band may still have limited capabilities for retrieving biomass from mature forest, but should be able to retrieve biomass in young and intermediate successional stages, and potentially more advanced stages as described by Vieira et al. (2003).

The final paper on land-cover mapping is presented by Souza, Firestone, Silva, and Roberts (2003), who describe a new approach for mapping degraded forests including burned and selectively logged forests. Souza et al. used SPOT-4 data to map forest degradation in Paragominas. Accuracy was assessed using two IKONOS images acquired in November 2000. They describe a multistage process for mapping degraded forest, starting with a forest/non-forest mask, followed by the use of SMA to map NPV, GV, soil and shade, and concluding with the use of a decision tree classifier to map logged and burned forest.

Ground reference data included forest inventories, which were used to relate spectral fractions to biophysical properties of forest degradation. Inventories included percentages of intact forest, woody debris, disturbed soil, burned vegetation, canopy cover, and total live and dead biomass. Spectral fractions showed that NPV, and shade increased in heavily burned areas. The main differences between heavily logged and burned forest were in the GV fraction. Logged forest showed decreased shade and a subtle increase in NPV. Regeneration following burning was characterized by an increase in GV and decrease in shade. Forest accounted for 57% of the area. However, of this area, only 20% was intact, with the remainder dominated by logged forest (32%). Degraded forest accounted for 5% of the area. NPV showed a linear, positive correlation with percent woody debris, and a negative, linear relationship to total biomass. This paper illustrates the importance of mapping degraded forests. In Paragominas, a majority of the area that might be considered intact forest is actually degraded. These conclusions are similar to the findings of a recent study by Alencar, Solórzano, and Nepstad (in press). Sensors such as TM or SPOT can be used to map degraded forests with reasonably high accuracies. The NPV fraction proved to be the most sensitive to forest degradation was found by Asner et al. for logged sites and was correlated with a number of biophysical characteristics, including woody debris and total biomass.

### 3.2. Land-cover characterization

Many of the papers described previously included some component of land-cover characterization as an element of mapping. The following papers focus primarily on using remote sensing to characterize surface properties, but do not focus on classifying the data. In the first paper, Asner, Bustamante, and Townsend (2003) evaluate image texture and SMA as means for quantifying sub-pixel and inter-pixel sources of variability in pasture. The authors introduce a new approach for estimating sub-pixel abundance from broadband data, called automated Monte Carlo unmixing (AutoMCU), in which end-members are selected randomly from a large bundle of acquired spectra as opposed to using a mean end-member spectrum. The study was conducted in the vicinity of Tapajós National Forest (Fig. 1). Texture was defined using a $3 \times 3$ window to calculate variance for TM bands 3–7. SMA was implemented using a spectral library developed from field spectra of soils, senesced pasture vegetation and small shrubs with spectra for large trees extracted from the image. Spectral fractions and estimates of error were calculated using AutoMCU to unmix each pixel repeatedly. Field data were used to place land-cover into seven categories based on quantitative cover estimates. Cover classes included agriculture, *campo limpo* (predominantly grass vegetation), *campo sujo* (defined as having >50% cover of short woody plants), three palm classes (10–30% palm, 30–70% palm, >70% palm) and *capoeira* (>80% forest regrowth <5 m height).

Image texture delineated cleared and forested lands. Cleared parcels had the highest variance in TM band 5, while closed canopy forest had the highest variance in TM band 4. Fractions derived using AutoMCU showed photosynthetic vegetation (PV, comparable to GV) to be highest in closed forest and lowest in agriculture and *campo limpo*. NPV was highest in *campo limpo*. When comparing variance to fractions, variance in the visible and shortwave infrared decreased with increasing PV and increased with increasing NPV. This paper demonstrates that AutoMCU, which was originally developed for hyperspectral data, is a viable approach for unmixing broadband multispectral data. Unlike deterministic models, it provides statistical measures that can be used to establish confidence limits for fractions without a strong dependence on the selection of a specific end-member. Clear, quantitative definitions of land-cover classes facilitate regional comparisons.

Asner and Warner (2003) analyzed 44 IKONOS scenes acquired across the region spanning a range of forest types. These scenes were analyzed to evaluate how shadow content and forest structure varied along a gradient of forest types ranging from dense tropical forest to tropical savanna (*cerrado*). Shadow fraction was determined using a thresholding technique applied to the panchromatic band. To evaluate how shadows impact red and NIR reflected radiance and the NDVI, a high-resolution shadow mask was resampled to 28 × 28 m to estimate percent shadow fraction within the equivalent of a Landsat pixel.

The authors documented considerable variation in shadow content in dense forest, averaging 25%, but ranging from 14% to 35%. Shadow content in savannas varied depending on density, ranging from a near zero for sparse woody vegetation to 12% for intermediate densities (25–75% woody vegetation) to an average of 16% for dense savanna (>75% woody vegetation). In forests and savannas, shadows had a significant impact on red reflected radiance, but only affected NIR radiance in forests. NDVI was only weakly affected by shadows except in the case of intermediate densities of woody vegetation in savanna. This study represents the first region-wide study to use high-resolution data to assess structurally related changes in shadow content for tropical forest and savanna, documenting the importance of shadow in tropical rainforest and how shadow affects reflected radiance.

Ferreira, Yoshioka, Huete, & Sano (2003) employ a multiscale approach to evaluate seasonal and sensor-dependent sensitivity of NDVI and the Enhanced Vegetation Index (EVI) to changes in *cerrado* vegetation under clear sky and turbid atmospheres. The study was conducted in the Brasília National Park. While few LBA projects have focused on *cerrado*, it is an important biome because it represents the largest region of neo-tropical savanna in the world and has the second largest area of all biomes in South America (Oliveira & Marquis, 2002). It experiences considerably greater seasonal variation in rainfall than the forest and has been subject to more rapid clearing (Klink & Moreira, 2002). NDVI and EVI were simulated for ETM+ MODIS, and AVHRR using airborne spectral data acquired by the MODLAND Quick Airborne Looks (MQUALS) package over five *cerrado* vegetation types, *cerrado* grassland, shrub *cerrado*, wooded *cerrado*, *cerrado* woodland, and gallery forest. Aircraft data were acquired during the wet (April/May) and dry (mid-July) seasons over the Brasília National Park. Field data included transects measuring percent cover, canopy height and tree spacing. Atmospheric contamination was evaluated at 10- and 100-km visibilities.

Both indices and first derivatives calculated from spectra were found to be linearly correlated with percent green cover. Of the sensors simulated, ETM+ had the best capability for monitoring seasonal dynamics, with AVHRR showing the poorest sensitivity. However, spectral indices captured only approximately half of the ground-based estimates of changes in greenness. In comparing indices, EVI proved to be superior to the NDVI, primarily because NDVI has a strong sensitivity to atmospheric contamination. MODIS EVI was the least sensitive to atmospheric contamination, followed by ETM+ EVI and AVHRR NDVI. The ability to quantify seasonal dynamics is critical for estimating net primary productivity. These results suggest that MODIS, or some combination of MODIS and ETM+ are sufficient for monitoring seasonal dynamics in *cerrado*. They also show the importance of developing transfer functions between sensors, to account for differences in the sensitivity to surface dynamics and atmospheric contamination. Transfer functions between MODIS and AVHRR, for example, are critical for linking current observations to historical measurements derived from AVHRR.

### 3.3. Land-use

The final paper, by Cardille and Foley (2003), fuses census and satellite land-cover data from the 1990s to generate spatially explicit maps showing agricultural land-use. These relationships were then exported to 1980 agricultural census data, and used to examine changes in land-use. The authors describe a model that uses 1995 land-cover data generated from the University of Maryland (UMd) and the 1995 Brazilian Agricultural Census to redistribute census-based estimates of land-use at the municipality level into a spatially explicit map of land-use. Three land-use categories were derived from the census data, cropland, natural pasture and planted pasture. The UMd and census data were fused using a regression tree that relates agricultural density to UMd land-cover categories. Once developed, the relationships were applied to the 1980 census data to map spatially explicit land-use in 1980.

Based on their analysis, the authors report a net increase in agricultural lands of 7 million ha between 1980 and 1995. Much of this increase occurred in planted pasture, which increased by 14.6 million ha, with a smaller increase in crop land, equal to 800,000 ha. Natural pasture decreased by 8.4 million ha over the same time period. The 7 million ha increase in active agriculture is considerably lower than most published accounts of deforestation between 1980 and 1995. The differences were reconciled by considering common reporting regions, removing natural pasture loss as a category and by accounting for pasture abandonment between 1980 and 1995. The authors hypothesized that steady state abandonment of pasture to second growth, which would be counted as deforestation, but excluded from their own land-use categories could account for a large proportion of the difference. Using a Markov model to simulate pasture abandonment, they determined that a steady state ratio of second growth to cleared lands of 36% when applied to pasture area mapped by INPE and the Tropical Rain Forest Information Center, bracketed their own estimate of planted pasture. This estimate of second growth is consistent with region-wide estimates of second growth (Lucas et al., 2000). This paper is significant because presents the first spatially explicit maps of agricultural land-use between 1980 and 1995 for the Brazilian Amazon.

## 4. Discussion

In this special issue, we include a subset of the remote sensing research that has occurred during LBA. Several themes dominate, including data set generation (Siqueira et al.; Hess et al.; Cardille and Foley; Ballester et al.), and land-cover mapping with an emphasis on second-growth forest (Lu et al.; Vieira et al.; Santos et al.). Other important issues, such as pasture sustainability and forest degradation are included in at least one paper (Numata et al.; Souza et al.). Several new techniques are introduced, including AutoMCU (Asner et al.), and several new approaches for mapping land-cover (Hess et al.; Lu et al.; Souza et al) as well as a promising approach for fusing census and remotely sensed data (Cardille and Foley). A diversity of sensors are utilized, including ETM+, IKONOS, SPOT-4, Airborne P-band SAR, and L-band SAR measured by JERS-1. Several papers include important, new field measures of species composition, forest structure and biomass in mature forest and secondary succession (Santos et al.; Vieira et al.). A common theme in more than half of the papers is quantitative definitions of land-cover and careful measures of map accuracy.

Early applications for a number of these data sets already show promise. For example, Siqueira et al. describe the development of a dual season mosaic, which is used by Hess et al. to map wetland vegetation and high and low water. Improved estimates of the large areas periodically flooded has already shown promise in improving our ability to estimate $CO_2$ outgassing from Amazonian waters (Richey et al., 2002). Ballester et al. use a combination of remote sensing and GIS to map land-cover and soil properties within a large watershed, evaluating how soil quality and pasture area effect river chemistry. Souza et al. provide a nice example from Paragominas, which shows that a majority of the area which might be considered forest, is actually degraded. New techniques, such as AutoMCU (Asner et al.), decision trees (Souza et al.), and SMA applied to mapping second growth (Lu et al.) have the potential of improving our ability to map land-cover and quantify change over large areas.

Several themes are likely to dominate the future research in LBA. A large number of new sensors, including MODIS, ASTER, Hyperion, and LIDAR are likely to see greater use. Analysis tools such as geostatistics, which enable researchers to fuse coarse- and fine-resolution data to produce maps that combine the strengths of multiple sensors are expected to provide new ways to characterize land cover. Improved quantification of damage by logging and burning forest degradation should result in an improved understanding of the importance of forest degradation. Mapping and monitoring of second-growth forests should continue to be refined. Data accessibility has improved considerably, making large area mapping over extended time series more feasible. Standardized remote sensing methodology (e.g., Roberts et al., 2002), quantitative descriptions of land cover and growing use of fine-resolution data for accuracy assessment (e.g., IKONOS or digital airborne videography; Hess et al., 2002) enhance the potential for interregional comparisons and the production of validated maps. The potential of many of these new land-cover maps for modeling has only just begun to be explored.

## Acknowledgements

We acknowledge Brazil's Ministry of Science and Technology (MCT) and its research institutions, the Instituto Nacional de Pesquisas de Amazônia (INPA) and the Instituto Nacional de Pesquisas Espacias (INPE), for leadership of LBA. The US National Aeronautics and Space Administration (NASA) and the Fundação de Amparo à Pesquisa do Estado de São Paulo (FAPESP) provided generous support for ecological research in LBA. Brazil's Conselho Nacional de Desenvolvimento Científico e Tecnológico (CNPq) provided many valuable fellowships to support students in LBA research. We are indebted to Drs. Diane Wickland, Tony Janetos, Jerry Melillo, Carlos Nobre, and Carlos Cerri for their early vision of ecological research in LBA. We thank Dr. Darrel Williams for his guidance in preparing this special issue and Dylan Prentiss for help in editing and the excellent support he provided in creating Fig. 1. Finally, we wish to thank the more than 30 reviewers who volunteered their time to review manuscripts for this special issue.

## References


Adams, J. B., Sabol, D., Kapos, V., Almeida Filho, R., Roberts, D. A., Smith, M. O., & Gillespie, A. R. (1995). Classification of multispectral images based on fractions of endmembers: Application to land-cover change in the Brazilian Amazon. *Remote Sens. Environ.*, *52*, 137–154.

Alencar, A. A. C., Solórzano, L. A., & Nepstad, D. C. (in press). Modeling forest understory fires under and eastern Amazonian landscape. *Ecol. Appl.*

Alves, D. S., Pereira, J. L. G., De Sousa, C. L., Soares, J. V., & Yamaguchi, F. (1999). Characterizing landscape changes in central Rondonia using Landsat TM imagery. *Int. J. Remote Sens.*, *20*(4), 2877–2882.

Alves, D. S., Soares, J. V., Amaral, S., Mello, E. M. K., Almeida, S. A. S., da Silva, O. F., & Silveira, A. M. (1997). Biomass of primary and secondary vegetation in Rondônia, Western Brazilian Amazon. *Glob. Chang. Biol.*, *3*, 451–461.

Angelis, C. F., Freitas, C. C., Valeriano, D. M., & Dutra, L. V. (2002). Multitemporal analysis of land-use/land-cover JERS-1 backscatter in the Brazilian Tropical Rainforest. *Int. J. Remote Sens.*, *23*(7), 1231–1240.

Asner, G. P., Bustamante, M. M. C., & Townsend, A. R. (2003). Scale dependence of biophysical structure in deforested areas bordering the Tapajós National Forest, Central Amazon. *Remote Sens. Environ., 87*, 507–520.

Asner, G. P., Keller, M., Pereira, R., & Zweede, J. C. (2002). Remote sensing of selective logging in Amazonia: Assessing limitations based on detailed field observations, Landsat ETM+ and textural analysis. *Remote Sens. Environ.*, *80*(3), 483–496.

Asner, G. P., Keller, M., Pereira Jr., R., Zweede, J. C., & Silva, J. N. M. (in press). Canopy damage and recovery following selective logging in an Amazon forest: Integrating field and satellite studies. *Ecol. Appl.*

Asner, G. P., Townsend, A. R., & Bustamante, M. C. (1999). Spectrometry of pasture condition and biogeochemistry in the Central Amazon. *Geophys. Res. Lett.*, *26*(17), 2769–2772.

Asner, G. P., Warner, A. S. (2003). Canopy shadow in IKONOS satellite observations of tropical forests and savannas. *Remote Sens. Environ., 87*, 521–533.

Avissar, R., & Nobre, C. A. (2002, Sep–Oct). Preface to special issue on the Large-Scale Biosphere–Atmosphere Experiment in Amazonia (LBA). *J. Geophys. Res.-Atmospheres*, *107*(D20), 8034.

Ballester, M. V. R., Victoria, D. de C., Krusche, A. V., Coburn, R., Victoria, R. L., Richey, J. E., Logsdon, M. G., Mayorga, E., & Matricardi, E. (2003). A remote sensing/GIS-based physical template to understand the biogeochemistry of the Ji-Paraná River basin (Western Amazônia). *Remote Sens. Environ., 87*, 429–445.

Biggs, T. W., Dunne, T., Domingues, T. F., & Martinelli, L. A. (2002). Relative influence of natural watershed properties and human disturbance on stream solute concentrations in the southwestern Brazilian Amazon basin. *Water Resour. Res.*, *38*(8), 1150.

Brown, I. F., Martinelli, L. A., Thomas, W. W., Moreira, M. Z., Ferreira, C. A. C., & Victoria, R. A. (1995). Uncertainty in the biomass of Amazonian forests: An example from Rondonia, Brazil. *For. Ecol. Manag.*, 175–189.

Brown, S., & Lugo, A. E. (1992). Aboveground biomass estimates for tropical moist forests of the Brazilian Amazon. *Interciencia*, *17*(1), 8–18.

Cardille, J. A., & Foley, J. A. (2003). Agricultural land-use change in Brazilian Amazônia between 1980 and 1995: Evidence from Integrated Satellite and Census data. *Remote Sens. Environ.,* 551–562.

Cochrane, M. A. (2001). Synergistic interactions between habitat fragmentation and fire in evergreen tropical forests. *Conserv. Biol.*, *15*(6), 1515–1521.

Cochrane, M. A., & Souza, C. M. (1998). Linear mixture model classification of burned forests in the eastern Amazon. *Int. J. Remote Sens.*, *19*(17), 3433–3440.

Cochrane, T. T., & Cochrance, T. A. (1998). SIGTERON, Sistema de Informação Geográfica para os terrenos e solos do Estado de Rondônia, Brail, Tecnosolo/DHV Consultants, Porto Velho, Rondônia.

Costa, M. P. F., Niemann, O., Novo, E., & Ahern, F. (2002). Biophysical properties and mapping of aquatic vegetation during the hydrological cycle of the Amazon floodplain using JERS-1 and Radarsat. *Int. J. Remote Sens.*, *23*(7), 1401–1426.

de Moraes, J. F. L., Seyler, F., Cerri, C., & Volkoff, B. (1998). Land-cover mapping and carbon pools estimates in Rondonia, Brazil. *Int. J. Remote Sens.*, *19*(5), 921–934.

EMBRAPA (1983). Mapa de levantamento de reconhecimento de média intenside does solos do Estado de Rondônia. Mapas 73, 74, 75 e 76, CEPA, RO.

Fearnside, P. M. (1993). Deforestation in Brazilian Amazonia: The effect of population and land tenure. *Ambio*, *22*(8), 537–545.

Fearnside, P. M. (1996). Amazonian deforestation and global warming: Carbon stocks in vegetation replacing Brazil's Amazon forest. *For. Ecol. Manag.*, *80*, 21–34.

Fearnside, P. M., & Salati, E. (1985). Explosive deforestation in Rondonia, Brazil. *Environ. Conserv.*, *12*(4), 355–356.

Ferreira, L. G., Yoshioka, H., Huete, A., & Sano, E. E. (2003). Seasonal landscape and spectral vegetation index dynamics in the Brazilian Cerrado: An analysis within the Large Scale Biosphere–Atmosphere Experiment in Amazônia (LBA). *Remote Sens. Environ., 87*, 534–550.

Foody, G. M., Palubinskas, G., Lucas, R. M., Curran, P. J., & Honzak, M. (1996). Identifying terrestrial carbon sinks: Classification of successional stages in regenerating tropical forest from Landsat TM data. *Remote Sens. Environ.*, *55*, 205–216.

Hansen, M. C., Defries, R. S., Townshend, J. R. G., & Sohlberg, R. (2000). Global land-cover classification at 1 km spatial resolution using a classification tree approach. *Int. J. Remote Sens.*, *21*(6–7), 1331–1364.

Hess, L. L., Melack, J. M., Filoso, S., & Wang, Y. (1995). Delineation of inundated area and vegetation along the Amazon floodplain with the SIR-C synthetic aperture radar. *IEEE Trans. Geosci. Remote Sens.*, *33*(4), 896–904.

Hess, L. L., Melack, J. M., Novo, E. M. L. M., Barbosa, C. C. F., & Gastil, M. (2003). Dual-season mapping of wetland inundation and vegetation for the Central Amazon region. *Remote Sens. Environ., 87*, 404–428.

Hess, L. L., Novo, E. L. M., Slaymaker, D. M., Holt, J., Steffen, C., Valeriano, D. M., Mertes, L. A. K., Krug, T., Melack, J. M., Gastil, M., Holmes, C., & Hayward, C. (2002). Geocoded digital videography for validation of land cover mapping in the Amazon Basin. *Int. J. Remote Sens.*, *23*(7), 1527–1555.

Houghton, R. A., Lawrence, K. T., Hackler, J. L., & Brown, S. (2001). The spatial distribution of forest biomass in the Brazilian Amazon: A comparison of estimates. *Glob. Chang. Biol.*, *7*(7), 731–746.

Houghton, R. A., Skole, D. L., Nobre, C. A., Hackler, J. L., Lawrence, K. T., & Chomentowski, W. H. (2000). Annual fluxes of carbon from deforestation and regrowth in the Brazilian Amazon. *Nature*, *403*, 301–304.

INMET (Instituto Nacional de Meteorologia) (1999). Map of annual rainfall isohyets for period 1931–1990 in Brazil. http://www.inmet.gov.br/.

INPE, Monitoramento da floresta Amazônica Brasileira por satélite 1998–1999 (2000). Instituto Nacional de Pesquisas Espaciais (22 pp.).

INPE, Monitoramento da floresta Amazônica Brasileira por satélite 1999–2001 (2003), www.dpi.inpe.br/prodesdigital, Instituto Nacional de Pesquisas Espaciais.

Johnson, C. M., Zarin, D. J., & Johnson, A. H. (2000). Post-disturbance aboveground biomass accumulation in global secondary forests: Climate, soil texture, and forest-type effects. *Ecology*, *81*(5), 1395–1401.

Junk, W. J., & Firch, K. (1985). The physical and chemical properties of Amazonian waters and their relationship with the biota. In G. T. Prance, & T. E. Lovejoy (Eds.), *Amazonia* (pp. 3–17). New York: Pergamon.

Keller, M., Alencar, A., & Asner, G. P., et al. (in press). Ecological research in the Large Scale Biosphere Atmosphere Experiment in Amazonia (LBA): A discussion of early results. *Ecol. Appl.*

Kimes, D. S., Nelson, R. F., Salas, W. A., & Skole, D. L. (1999). Mapping secondary tropical forest and forest age from SPOT HRV data. *Int. J. Remote Sens.*, *20*(18), 3625–3640.

Klink, C. A., & Moreira, A. G. (2002). Past and current human occupation, and land-use. In P. S. Oliveira, & R. J. Marquis (Eds.), *The cerrados of Brazil* (pp. 69–88). New York, NY, USA: Columbia Univ. Press.

Laurance, W. F., Ferreira, L. V., Rankin-de Merona, J. M., & Laurance, S. G. (1998). Rain forest fragmentation and the dynamics of Amazonian tree communities. *Ecology*, *79*(6), 2032–2040.

Lean, J., & Rowntree, P. (1993). A GCM simulation of the impact of Amazonian deforestation on climate using an improved canopy representation. *Q. J. R. Meteorol. Soc.*, *119*, 509–530.

Loveland, T. R., Reed, B. C., Brown, J. F., Ohlen, D. O., Zhu, Z., Yang, L., & Merchant, J. W. (2000). Development of a global land cover characteristics database and IGBP DISCover from 1 km AVHRR Data. *Int. J. Remote Sens.*, *21*, 1303–1330.

Lu, D., Moran, E., Batistella, M. (2003). Linear mixture model applied to Amazonian vegetation classification. *Remote Sens. Environ., 87*, 456–469.

Lucas, R. M., Honzak, M., Curran, P. J., Foody, G. M., Milnes, R., Brown, T., & Amaral, S. (2000). Mapping the regional extent of tropical forest regeneration stages in the Brazilian Legal Amazon using NOAA AVHRR data. *Int. J. Remote Sens.*, *21*(15), 2855–2881.

Lucas, R. M., Honzak, M., do Amaral, I., Curran, P. J., & Foody, G. M. (2002). Forest regeneration on abandoned clearances in Central Amazonia. *Int. J. Remote Sens.*, *23*(5), 965–988.

Lucas, R. M., Honzak, M., Foody, G. M., Curran, P. J., & Corves, C. (1993). Characterizing tropical secondary forests using multi-temporal Landsat sensor imagery. *Int. J. Remote Sens.*, *14*(16), 3061–3067.

Malingreau, J. P., & Tucker, C. J. (1990). Ranching in the Amazon region: Large-scale changes observed by AVHRR. *Int. J. Remote Sens.*, *11*(2), 187–189.

Marengo, J. A., & Nobre, C. A. (2001). General characteristics and variability of climate in the Amazon Basin and its links to the global climate system. In M. E. McClain, R. L. Victoria, & J. E. Richey (Eds.), *The biogeochemistry of the Amazon Basin*. New York, NY, USA: Oxford Univ. Press.

Moran, E. F., Brondizio, E., Mausel, P., & Wu, Y. (1994). Integrating Amazonian vegetation, land-use, and satellite data. *Bioscience*, *44*(5), 329–338.

Moran, E. F., Brondizio, E. S., Tucker, J. M., da Silva-Forsberg, M. C., McCracken, S., & Falesi, I. (2000). Effects of soil fertility and land-use on forest succession in Amazônia. *For. Ecol. Manag.*, *139*, 93–108.

Nelson, R. F., Kimes, D. S., Salas, W. A., & Routhier, M. (2000). Secondary forest age and tropical forest biomass estimation using Thematic Mapper imagery. *Bioscience*, *50*(5), 419–431.

Nepstad, D. C., Verissimo, J. A., Alencar, A., Nobre, C., Lima, E., Lefebvre, P., Schlesinger, P., Potter, C., Moutinho, P., Mendoza, E., Cochrane, M., & Brooks, V. (1999). Large-scale impoverishment of Amazonian forests by logging and fire. *Nature*, *398*, 505–508.

Nobre, C. A., Sellers, P. J., & Shukla, J. (1991). Amazonian deforestation and regional climate change. *J. Clim.*, *4*, 957–988.

Novo, E. M. L. M., Costa, M. P. F., Mantovani, J. E., & Lima, I. B. T. (2002). Relationship between macrophyte stand variables and radar backscatter at L and C band, Tucuruí Reservoir, Brazil. *Int. J. Remote Sens.*, *23*(7), 1241–1260.

Numata, I., Soares, J. V., Roberts, D. A., Leonidas, F. C., Chadwick, O. A., & Batista, G.T. (2003). Relationships among soil fertility dynamics and remotely sensed measures across pasture chronosequences in Rondônia, Brazil. *Remote Sens. Environ., 87*, 446–455.

Oliveira, P. S., & Marquis, R. J. (Eds.) (2002). *The Cerrados of Brazil—ecology and natural history of a neotropical Savanna*. New York, NY, USA: Columbia University Press.

Pereira, R., Zweede, J., Asner, G. P., & Keller, M. (2002). Forest canopy damage and recovery in reduced-impact and conventional selective logging in Eastern Para, Brazil. *For. Ecol. Manag.*, *168*, 77–89.

Potter, C. S., Randerson, J. T., Field, C. B., Matson, P.A, Vitousek, P. M., Mooney, H. A., & Klooster, S. A. (1993). Terrestrial ecosystem production: A process model based on global satellite and surface data. *Glob. Biogeochem. Cycles*, *7*(4), 811–841.

Richey, J. E., Melack, J. M., Aufdenkampe, A. K., Ballester, V. M., & Hess, L. L. (2002). Outgassing from Amazonian rivers and wetlands as a large tropical source of atmospheric $CO_2$. *Nature*, *416*, 617–620.

Rignot, E., Salas, W. A., & Skole, D. L. (1997). Mapping deforestation and secondary growth in Rondônia, Brazil, using imaging radar and Thematic Mapper data. *Remote Sens. Environ.*, *59*, 167–179.

Roberts, D. A., Batista, G., Pereira, J., Waller, E., & Nelson, B. (1998). Change identification using multitemporal spectral mixture analysis: Applications in Eastern Amazonia. In C. Elvidge, & R. Lunetta (Eds.), *Remote sensing change detection: Environmental monitoring applications and methods* (pp. 137–161). Ann Arbor, MI: Ann Arbor Press, Chapter 9.

Roberts, D. A., Numata, I., Holmes, K., Batista, G., Krug, T., Monteiro, A., Powell, B., & Chadwick, O. A. (2002). Large area mapping of land-cover change in Rondonia using multitemporal Spectral Mixture Analysis and decision tree classifiers. *J. Geophys. Res.*, *107*(D20), 8073.

Running, S. W., Baldocchi, D. D., Turner, D. P., Gower, S. T., Bakwin, P. S., & Hibbard, K. A. (1999). A global terrestrial monitoring network integrating tower fluxes, flask sampling, ecosystem modeling and EOS satellite data. *Remote Sens. Environ.*, *70*(1), 108–127.

Saatchi, S. S., Nelson, B., Podest, E., & Holt, J. (2000). Mapping land-cover types in the Amazon Region using 1 km JERS-1 mosaic. *Int. J. Remote Sens.*, *21*(6–7), 1201–1234.

Salas, W. A., Ducey, M. J., Rignot, E., & Skole, D. (2002a). Assessment of JERS-1 SAR for monitoring secondary vegetation in Amazonia: I. Spatial and temporal variability in backscatter across a chronosequence of secondary vegetation stands in Rondonia. *Int. J. Remote Sens.*, *23*(7), 1357–1380.

Salas, W. A., Ducey, M. J., Rignot, E., & Skole, D. (2002b). Assessment of JERS-1 SAR for monitoring secondary vegetation in Amazonia: II. Spatial, temporal and radiometric consideration for operational monitoring. *Int. J. Remote Sens.*, *23*(7), 1381–1400.

Salati, E. (1985). The climatology and hydrology of Amazonia. *Amazonia* (pp. 18–48). New York: Pergamon.

Salati, E., & Vose, P. B. (1984). Amazon Basin: A system in equilibrium. *Science*, *225*, 129–138.

Santos, J. R., Freitas, C. C., Araujo, L. S., Dutra, L. V., Mura, J. C., Gama, F. F., Soler, L. S., & Sant'Anna, S. J. S. (2003). Airborne P-band SAR applied to the above ground biomass studies in the Brazilian tropical rainforest. *Remote Sens. Environ., 87*, 482–493.

Sippel, S., Hamilton, S. K., Melack, J. M., & Choudhury, B. J. (1994). Determination of inundation area in the Amazon river floodplain using the SMMR 37 GHz polarization difference. *Remote Sens. Environ.*, *48*, 70–76.

Siqueira, P., Chapman, B., & McGarragh, G. (2003). The coregistration, calibration and interpretation of the multiseason JERS-1 SAR data over South America. *Remote Sens. Environ., 87*, 389–403.

Skole, D., & Tucker, C. (1993). Tropical deforestation and habitat fragmentation in the Amazon: Satellite data from 1978 to 1988. *Science*, *260*, 1905–1910.

Skole, D. L., Chomentowski, W. H., & Salas, W. H. (1994). Physical and human dimensions of deforestation in Amazonia. *Bioscience*, *44*(5), 314–322.

Souza, C., & Barreto, P. (2000). An alternative approach for detecting and monitoring selectively logged forests in the Amazon. *Int. J. Remote Sens.*, *21*(1), 173–179.

Souza, Jr., C., Firestone, L., Silva, L. M., & Roberts, D. (2003). Mapping forest degradation in the Eastern Amazon from SPOT 4 through Spectral Mixture Models. *Remote Sens. Environ., 87*, 494–506.

Steininger, M. K. (1996). Tropical secondary forest regrowth in the Amazon: Area, age and change estimation with Thematic Mapper data. *Int. J. Remote Sens.*, *17*, 9–27.

Steininger, M. K. (2000). Satellite estimation of tropical secondary forest above-ground biomass: Data from Brazil and Bolivia. *Int. J. Remote Sens.*, *21*, 1139–1159.

Steininger, M. K., Tucker, C. J., Townshend, J. R. G., Killeen, T. J., Desch, A., Bell, V., & Ersts, P. (2001). Tropical deforestation in the Bolivian Amazon. *Environ. Conserv.*, *28*(2), 127–134.

Stone, T. A., & Lefebvre, P. A. (1998). Using multi-temporal satellite data to evaluate selective logging in Para, Brazil. *Int. J. Remote Sens.*, *13*, 2517–2526.

Stone, T. A., Schlesinger, P., Houghton, R. A., & Woodwell, G. M. (1994). A map of vegetation of South America based on satellite imagery. *Photogramm. Eng. Remote Sensing*, *60*(5), 541–551.

Uhl, C., & Vieira, I. C. G. (1989). Ecological impacts of selective logging in the Brazilian Amazon, a case study from the Paragominas region of the state of Para. *Biotropica*, *21*(2), 98–106.

Vieira, I. C. G., de Almeida, A. S., Davidson, E. A., Stone, T. A., de Carvalho, C. J. R., & Guerrero, J. B. (2003). Classifying successional forests using Landsat spectral properties and ecological characteristics in Eastern Amazônia. *Remote Sens. Environ., 87*, 470–481.